Hindawi Publishing Corporation
Advances in Biomaterials
Volume 2014, Article ID 697491, 13 pages
http://dx.doi.org/10.1155/2014/697491

Research Article

In Vitro Corrosion Studies of Surface Modified NiTi Alloy for Biomedical Applications

Manju Chembath,[1] J. N. Balaraju,[1] and M. Sujata[2]

[1] *Surface Engineering Division, CSIR National Aerospace Laboratories, Post Bag No. 1779, Bangalore, Karnataka 560017, India*
[2] *Materials Science Division, CSIR National Aerospace Laboratories, Post Bag No. 1779, Bangalore, Karnataka 560017, India*

Correspondence should be addressed to J. N. Balaraju; jnbalaraju@rediffmail.com

Received 30 June 2014; Revised 1 October 2014; Accepted 21 October 2014; Published 20 November 2014

Academic Editor: William A. Brantley

Electropolishing was conducted on NiTi alloy of composition 49.1 Ti-50.9 Ni at.% under potentiostatic regime at ambient temperature using perchloric acid based electrolyte for 30 sec followed by passivation treatment in an inorganic electrolyte. The corrosion resistance and biocompatibility of the electropolished and passivated alloys were evaluated and compared with mechanically polished alloy. Various characterization techniques like scanning electron microscopy, atomic force microscopy, and X-ray photoelectron spectroscopy were employed to analyze the properties of surface modified and mechanically polished alloys. Water contact angle measurements made on the passivated alloy after electropolishing showed a contact angle of 35.6°, which was about 58% lower compared to mechanically polished sample, implying more hydrophilicity. The electrochemical impedance studies showed that, for the passivated alloy, threefold increase in the barrier layer resistance was obtained when compared to electropolished alloy due to the formation of compact titanium oxide. The oxide layer thickness of the passivated samples was almost 18 times higher than electropolished samples. After 14 days immersion in Hanks' solution, the amount of nickel released was 315 ppb which was nearly half of that obtained for mechanically polished NiTi alloy, confirming better stability of the passive layer.

1. Introduction

Binary NiTi alloys containing 50-51 at.% Ni are widely used for biomedical applications owing to their unique shape memory as well as superelastic properties and are preferred over conventional implant materials like Co-Cr-Mo alloys and stainless steel for specific applications [1]. These alloys are reported to exhibit surface passivity due to the presence of native titanium oxide layer which prevents the alloy from corrosion under the influence of body fluids and hence they possess superior biocompatibility compared to stainless steel [2, 3]. In spite of its remarkable properties, nickel elution is still a major issue of concern in using NiTi alloys, as high nickel content creates serious health hazards when implanted into human body. Human physiological environment is complex and the biocompatibility of the material needs to be established prior to use as an implant device. Nickel elution on immersion of NiTi in simulated body fluids (SBF) has been studied by various researchers [4–6]. Since nickel elution produces severe allergic issues, many of the research works on NiTi alloys were focused on improving the biocompatibility and corrosion resistance by suitable surface modification techniques [7–9]. The corrosion behavior of the alloy has been analyzed in various simulated body fluids such as Tyrode's, Hanks', phosphate buffered saline (PBS), and 0.9 wt.% NaCl solutions [10–17]. Results of these studies showed that the electrochemical behavior and the nickel release rate vary from one type of solution to the other although the chloride content in these physiological solutions remained almost the same. Therefore the presence of other ions also plays a significant role in the electrochemical behavior of NiTi. The purity and ratio of individual elements, method of melting/casting [18], and shape memory heat treatment also play a vital role in determining the biocompatibility. The formation of uniform, compact, and defect free oxide on the surface was found to be beneficial in the place

of a thicker oxide layer [19]. Since the corrosion resistance of an alloy depends strongly on the surface structure and the composition, selective tuning of the surface of the alloy using chemical or electrochemical methods is expected to improve its corrosion resistance.

Among the various surface modification techniques developed so far for NiTi alloys, electropolishing process was proved to be beneficial, as it removes the outermost surface layer of the alloy formed during metal working operations and is effective in reducing the surface roughness from micro- to nanometer level, enabling the surface to function as a biomaterial [20, 21]. Electropolishing of NiTi alloys in various solutions has been developed and was found to improve the bioapplicability [22, 23]. These processes can be operated potentiostatically or galvanostatically at or below room temperature.

In the present study, the effect of electropolishing and passivation on the corrosion resistance of biomedical grade NiTi alloy has been carried out. Low temperature electropolishing treatments are generally preferred for obtaining good surface finish. The present work is focused on electropolishing of NiTi alloy in perchloric acid based solutions at ambient conditions for 30 sec, which we consider as the lowest duration compared to the literature reports [12, 24]. Electropolishing process was followed by passivation treatment in potassium periodate to form a passive film. The oxidizing power of potassium periodate is utilized for various applications [25]. Hence, passivation using periodate solution was expected to modify the surface properties of NiTi alloy also. Mechanism of electropolishing and passivation and their *in vitro* corrosion resistance and biocompatibility have been analyzed and compared to those of mechanically polished NiTi alloy.

2. Experimental

Vacuum arc melted and hot-rolled NiTi strips (50.9 at.% Ni) of 10 mm width and 1 mm thickness were employed in this study. The microstructure of NiTi alloy strip after etching in Kroll's reagent (HF, HNO_3, and H_2O in the ratio 5 : 3 : 92) was examined under secondary electron mode using scanning electron microscope (SEM, Carl Zeiss, Supra 40 VP). The composition of the phases present in the alloy was analyzed using a CAMECA Electron Probe Micro Analyzer (EPMA).

The specimens of dimension 10 mm × 10 mm × 1 mm were abraded progressively using SiC grinding papers from 100 to 600 grit and then ultrasonically cleaned in acetone and distilled water separately for 15 min. After being air dried, the samples were electropolished at a constant voltage for 30 s at room temperature in an electrolytic cell using stainless steel as cathode. The electrolyte consisted of perchloric acid, butanol, and absolute alcohol in the ratio 1 : 3 : 1. The voltages used for electropolishing (EP) were 15, 20, and 25 V. After electropolishing, the samples were ultrasonically cleaned in acetone and distilled water consecutively for 15 min. and air dried. Further, passivation treatment using potassium periodate was given to selected specimens. The sample identification shown in Table 1 will be followed in this paper unless otherwise stated.

Table 1: Details of sample identification and surface treatment conditions.

Sample identification	Surface treatment
Bare NiTi	Mechanically polished NiTi alloy
EP20V	Mechanical polishing followed by electropolishing at 20 V
EP20VPIE	Mechanical polishing and electropolishing at 20 V followed by passivation treatment using saturated potassium periodate solution at 95°C for 1 h.

The mean roughness factor, R_a, of mechanically and electropolished alloys was measured over a length of 3.1 mm using a profilometer (Surtronic 3+, Taylor Hobson make). The surface topography and roughness analysis for as-polished, electropolished, and passivated samples were characterized using atomic force microscopy (AFM, model SSI, CSEM make) under noncontact mode. The profile view of the sample was examined using nano profilometer. For all the samples, images were recorded over an area of 1.5 × 1.5 μm^2. Water contact angle of the samples was measured by sessile drop method using a Contact Angle Analyzer (model Phoenix 300 Plus from M/s Surface Electro Optics, South Korea). Deionized water with a droplet volume of 8 μL was dripped on the sample surface and the contact angle between the drop and the substrate was measured. The surface morphology of mechanically polished, electropolished, and passivated samples was examined using scanning electron microscope (Carl Zeiss, Supra 40 VP). Surface analysis was performed by an X-ray photoelectron spectrometer (SPECS) equipped with a hemispherical analyzer. The X-ray source used was Al Kα radiation with a pass energy of 20 eV. A vacuum generator argon source having a pressure of 10^{-9} Torr was used for sputtering. The spectra for each sample were generated after 2 minutes of argon sputtering and the binding energies were computed with reference to C1s peak located at 284.5 eV. For all the analyses, three samples were tested.

The electrochemical methods employed to evaluate the behavior of mechanically polished and surface-treated NiTi alloys include potentiodynamic polarization and electrochemical impedance spectroscopy (EIS) using CHI604D electrochemical workstation. The corrosion cell was first cleaned with deionized water, rinsed with phosphate buffered saline (PBS) solution, and filled with approximately 260 mL of PBS. The cell with its contents was brought up to 37°C by placing it in a controlled temperature water bath. The PBS solution was purged with ultrahigh-purity nitrogen for 30 min prior to immersion of the specimen. After immersion, nitrogen purging continued for an additional 30 min before starting the polarization tests. A saturated calomel electrode was used as the reference electrode and it was inserted into a Luggin Capillary. The surface area of the specimen in

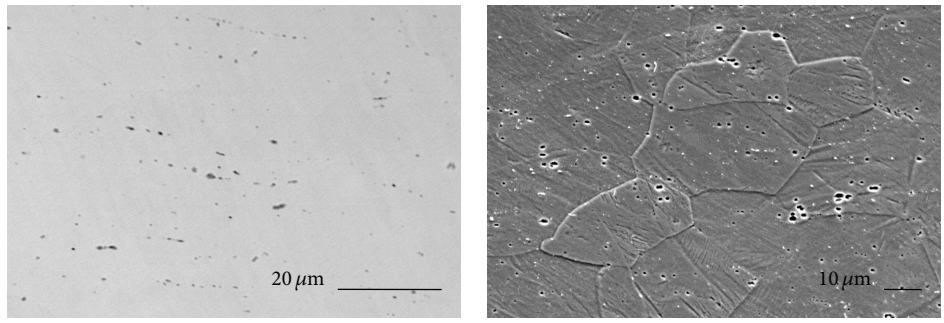

(a) (b)

Figure 1: Secondary electron microstructures of the cross-section of NiTi strip (a) unetched and (b) etched in Kroll's reagent.

contact with PBS was carefully calculated to increase the accuracy of the corrosion parameters. Polarization scans were performed at a rate of 0.167 mVs^{-1}. Corrosion current (E_{corr}) and corrosion current density (i_{corr}) were estimated by Tafel extrapolation to the cathodic and anodic part of the polarization curves, respectively. Corrosion rate was calculated as per ASTM G102 – 89 which is given as

$$\text{Corrosion rate, } C = \frac{(K \times i_{corr} \times EW)}{\rho}. \quad (1)$$

K = a constant given by 3.27×10^{-3} mm·g/μA·cm·year, i_{corr} = corrosion current density in $\mu A/cm^2$, EW = equivalent weight of NiTi alloy in grams, and ρ = density of NiTi in g/cm^3.

All the experiments were repeated thrice to check the repeatability.

The effect of surface modification on the metal ion release was assessed by measuring the amount of nickel released after immersion in Hanks' solution. The samples were kept in 5 mL of Hanks' solution and incubated in a thermostatic chamber at 37°C for 2 weeks. The solutions were periodically withdrawn and replaced with fresh solution. Nickel eluted out was quantitatively measured using atomic absorption spectrophotometer (AAS, GBC Scientific Equipment Ltd.).

The composition of PBS and Hanks' solution is given in Table 2.

Table 2: Composition of simulated body fluids used in the present study.

Chemicals	PBS (g/L)	Hanks' (g/L)
NaCl	8	8
$CaCl_2$		0.14
KCl	0.2	0.4
$MgCl_2 \cdot 6H_2O$		0.1
$MgSO_4 \cdot 7H_2O$		0.1
$NaHCO_3$		0.35
Na_2HPO_4	1.15	
$Na_2HPO_4 \cdot 2H_2O$		0.12
KH_2PO_4	0.2	0.06
Glucose		1

3. Results and Discussion

3.1. Substrate Characteristics. Secondary electron micrographs of polished and etched NiTi samples showed that the structure consisted of uniformly distributed particles/precipitates of size 1-2 μm in a matrix of polycrystalline NiTi grains (Figure 1(a)). EPMA analysis conducted on the second phase particles showed that they were Ti-enriched, with an approximate composition corresponding to Ti_2Ni. The average size of the NiTi grains was measured to be 30 μm (Figure 1(b)).

Electropolishing process was optimized at 20 V for 30 sec. Based on visual observations, it was found that, below and above this voltage, electropolishing was not efficient. At an applied voltage of 15 V, electropolished surface appeared dull whereas, at 25 V, the surface appeared bright but was found to be rough with large number of undulations and wavy pattern. Secondary electron micrographs depicting the morphology of mechanically polished, electropolished, and passivated NiTi samples were given in Figure 2. Scratches and grooves due to mechanical polishing were seen clearly in bare NiTi. After electropolishing at 20 V, the surface appeared smoother and the polishing marks were completely eliminated. Surface of the passivated sample appeared dull compared to electropolished sample possibly due to the formation of oxide layer.

3.2. Topography and Wetting Behavior. Studies revealed that surface roughness has a strong influence on the corrosion resistance of NiTi implant materials [26, 27]. The roughness values obtained in the present study for the untreated, electropolished, and passivated samples were given in Table 3.

The mechanically polished (bare) sample exhibited an average roughness of 76.8 nm. R_a value obtained for the electropolished and passivated sample using profilometer was 66.2 and 151.2 nm, respectively. The average roughness values obtained from AFM for mechanically polished NiTi, EP20V, and EP20VPIE were 1.7 nm, 2.5 nm, and 30.8 nm, respectively. The increase in roughness value after passivation could be due to the formation of titanium oxide at the surface.

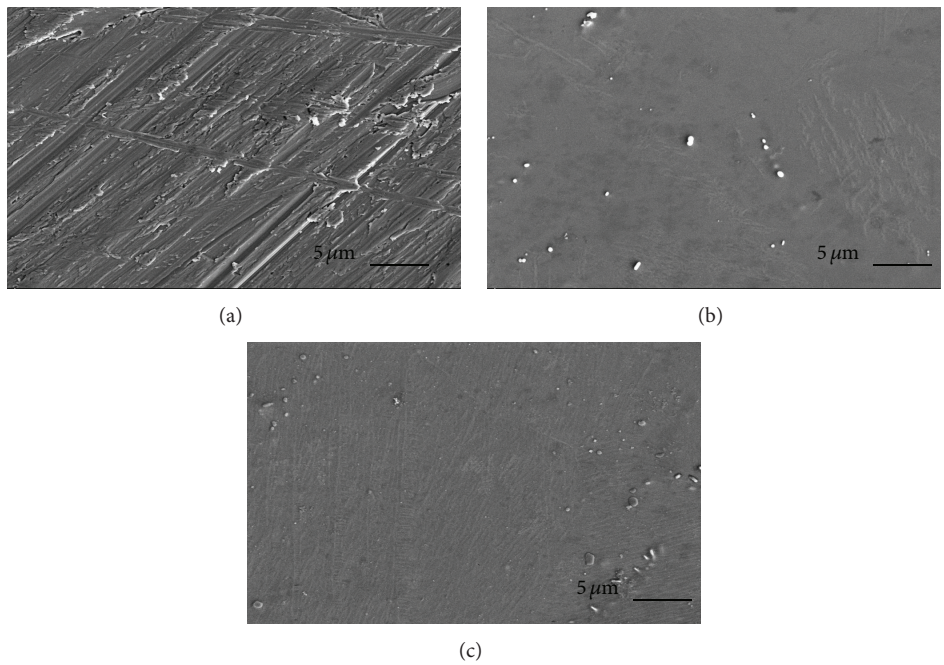

(a) (b) (c)

Figure 2: Surface morphology of (a) bare NiTi, (b) EP20V, and (c) EP20VPIE.

Table 3: Average surface roughness values of various NiTi samples from surface profilometer and AFM measurements.

Sample	Surface roughness, R_a (nm)	
	Profilometry	AFM
Bare NiTi	76.8 ± 6.8	1.7 ± 0.1
EP20V	66.2 ± 5.2	2.5 ± 1.2
EP20VPIE	151.2 ± 13.1	30.8 ± 2.4

The topographical images of untreated and surface modified NiTi alloy obtained using AFM are shown in Figures 3(a)–3(c).

Nonuniform "streaky" pattern was clearly visible for untreated sample which was due to mechanical polishing. After electropolishing at 20 V, there was a noticeable change in the topography of the surface, wherein it appeared as uniform distribution of nanospikes over the entire area. The topography of the passivated sample exhibited several bright nodules which have resulted due to modification of the surface during interaction with the electrolyte. These samples displayed more than twelve-fold increase in roughness compared to electropolished samples. These results were quantitatively in agreement with profilometry measurement (Figures 4(a)–4(c)).

There was a mismatch in the R_a values obtained using AFM and profilometer, the values being higher in the latter case. However, the trend in changes in the surface roughness due to surface modification was found similar irrespective of the technique used for measurement. It may be noted that there is a marginal change in the R_a values due to electropolishing. On the other hand, passivation was found to result in substantial increase in R_a values. While the increase was found to be nearly 2.5 times in the case of profilometry, AFM measurements indicated almost 12-fold increase in the surface roughness. The difference in the mismatch of R_a values obtained in the two techniques used could be attributed to scan length/area used for measurements. In the present study, the scan length for profilometric measurements and AFM was 3.1 mm and 1.5 μm, respectively. Longer scan lengths appeared to have resulted in a higher roughness value. Similar observations were mentioned by Eliaz and Nissan in the case of stainless steel [28]. In addition to the initial surface conditioning, the R_a value was found to be dependent on the magnitude of the surface area measured. Hence a diverse range of R_a values was reported in the literature for electropolished NiTi alloys [10, 12, 19]. The roughness value obtained from AFM was found to be 23.2 nm after electropolishing in perchloric acid solution when measurements were conducted over an area of $50 \times 50\ \mu m^2$ [12]. On the other hand, Cisse et al. reported slightly lower roughness value (1.7 nm) when the scan area was limited to $2 \times 2\ \mu m^2$ [19].

Graphical representation of contact angle observed for different samples studied was given in Figure 5. Contact angle of the mechanically polished (bare NiTi) sample was 85.6°. Electropolishing at 20 V showed a contact angle similar to that of mechanically polished samples. A significant change in the wetting behavior of the alloy was noticed after passivation process wherein the contact angle observed was 35.6°, which was about 58% lower compared to bare NiTi, indicating more hydrophilicity.

One of the necessary criteria for a biocompatible material is that the surface should have good wetting properties [29, 30]. The marked lowering of contact angle exhibited by the passivated alloy relative to other surfaces may be attributed

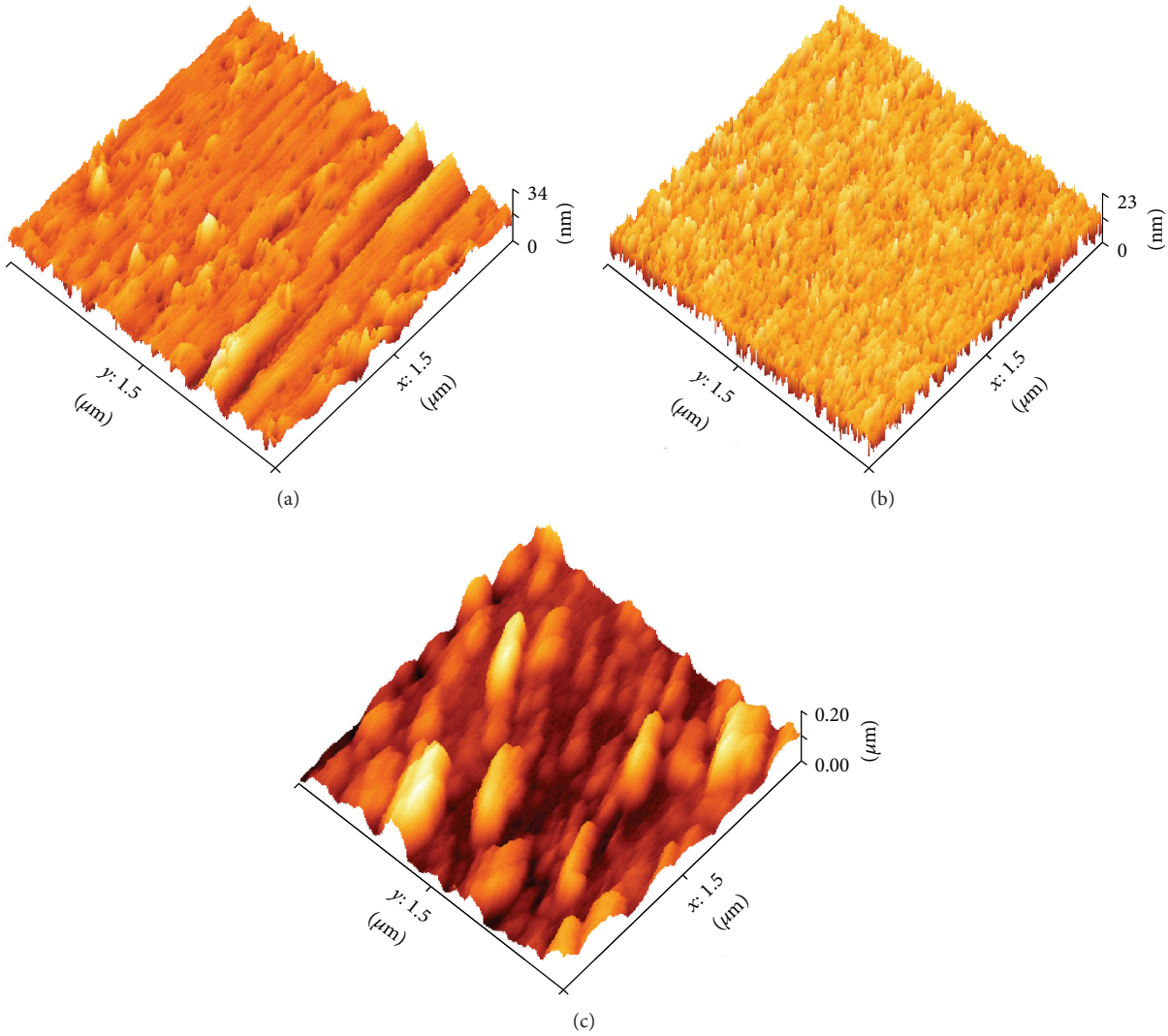

Figure 3: AFM images of various surface treated NiTi alloys: (a) bare NiTi, (b) EP20V, and (c) EP20VPIE.

to the transition of metal topography, namely, formation of oxide associated with pores and enhanced roughness [31–33]. In the current investigation, AFM image (Figure 3(c)) and the profile view (Figure 4(c)) support the formation of microsized nodules over these surfaces compared to electropolished samples. Based on the above, it can be concluded that the wettability of NiTi can be improved by potassium periodate passivation treatment.

3.3. Surface Analysis. Figure 6 depicts the XPS survey spectrum of mechanically polished sample which was almost identical to that of surface modified samples. The presence of Ni, Ti, O, and some amount of carbon due to physical adsorption of carbon containing molecules from the atmosphere was identified.

Surface chemical concentration of each element was given in Table 4. The nickel content was around 11% at the surface for bare NiTi which reduced to 0.8% after passivation. The Ti/Ni ratio for bare NiTi after sputtering was 1.8. Electropolishing process resulted in increasing the ratio to 3.8. However, after periodate treatment, the Ti/Ni ratio was found to be 30.1. Among all the samples, the surface concentration of nickel was the least for the passivated sample. Hence, it can be conjectured that electropolishing followed by passivation assists in reducing the content of nickel over the surface due to preferential oxidation of titanium to titanium dioxide.

Table 4: Atomic concentration of Ni and Ti for untreated and surface treated NiTi alloys from XPS data.

Sample	Ti (at.%)	Ni (at.%)	O (at.%)	Ti/Ni ratio
Bare NiTi	19.1	10.6	70.3	1.8
EP20V	26.9	7.1	66.0	3.8
EP20VPIE	24.1	0.8	75.1	30.1

Figures 7(a)–7(c) showed detailed Ti 2p spectra for all the three samples. The main peak at 458.7 eV could be assigned to Ti $2p_{3/2}$ in +4 oxidation state. The doublet separation was 6.1 eV. For bare and electropolished sample, a low intense peak at 454.6 eV was due to the presence

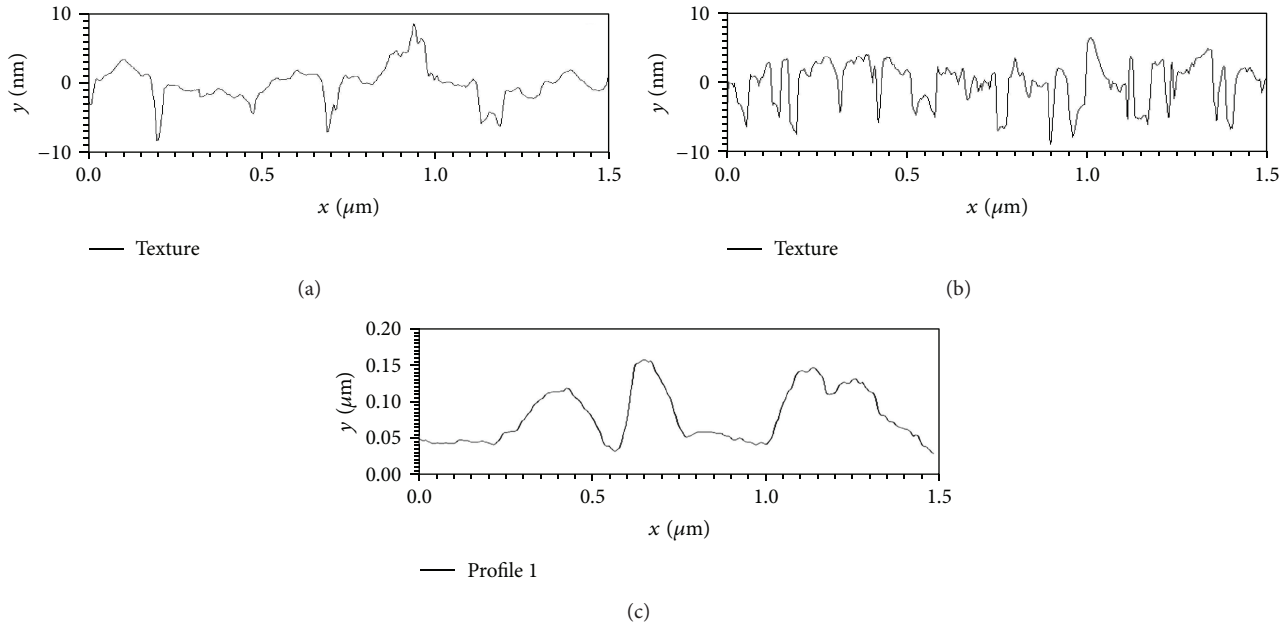

Figure 4: Profile view of various surface treated NiTi alloys: (a) bare NiTi, (b) EP20V, and (c) EP20VPIE.

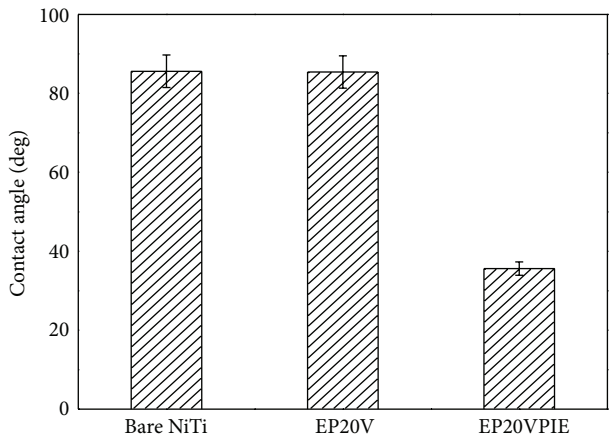

Figure 5: Variation of the contact angles observed in bare and surface modified NiTi samples.

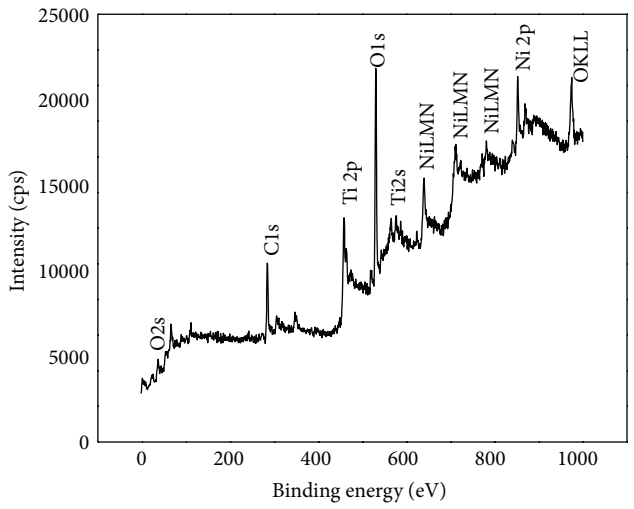

Figure 6: XPS survey spectrum for mechanically polished NiTi.

of unoxidized titanium present in the NiTi alloy. For this sample, existence of titanium in metallic state would result in reduced thickness of the passive layer as quoted by Vojtěch et al. [34]. After passivation, the corresponding peak was absent due to the complete oxidation of titanium under the experimental conditions. The thickness and compactness were expected to be more due to passivation treatment.

The high resolution photoelectron spectra of nickel in the 2p region for mechanically polished, electropolished, and passivated samples were given in Figures 8(a)–8(c). The spectra of bare NiTi and electropolished sample looked almost similar. The prominent peak at 852.3 eV could be attributed to the binding energy of Ni $2p_{3/2}$ in the elemental form. The spin orbit separation of $2p_{3/2}$ and $2p_{1/2}$ was 17.1 eV. A satellite peak at 859.3 eV which is the characteristics of Ni $2p_{3/2}$ was also seen in the figure. For passivated sample the peaks were noisy due to low concentration of nickel at the surface. Consequently nickel might have diffused inwards during the passivation process [35]. The absence of peak for nickel in +2 oxidation states and the selective oxidation of titanium are in accordance with the Gibbs free energies for the formation of NiO and TiO_2, which are −211.7 and −888.8 kJmol^{-1}, respectively [36].

3.4. Electrochemical Behavior. Potentiodynamic polarization curves obtained for mechanically polished and surface modified NiTi specimens in PBS solution were displayed in Figure 9 and the parameters were given in Table 5.

Table 5: Potentiodynamic polarization results of untreated and treated alloys.

Sample	E_{corr} (mV)	I_{corr} (nA/cm^2)	E_b (mV)	I_b (μA/cm^2)	Corrosion rate (mm/year)
Bare NiTi	−470 ± 28	770 ± 36	490 ± 35	19 ± 0.7	6.98×10^{-3}
EP20V	−292 ± 14	6 ± 0.3	1142 ± 78	4.2 ± 0.1	5.35×10^{-5}
EP20VPIE	−215± 15	5 ± 0.3	1010 ± 70	0.36 ± 0.08	4.26×10^{-5}

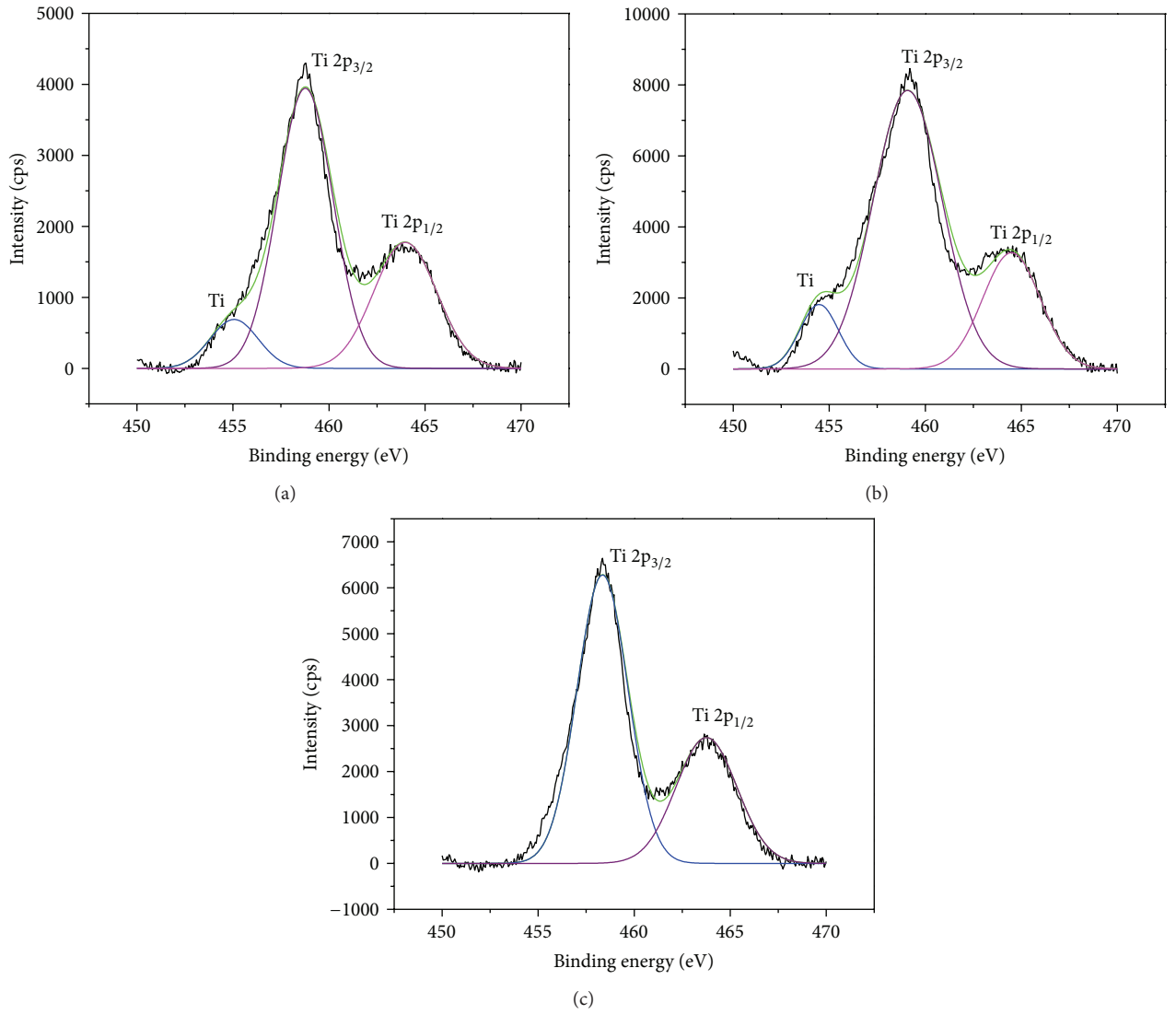

Figure 7: High resolution XPS spectra for Ti 2p region: (a) bare NiTi, (b) EP20V, and (c) EP20VPIE.

Corrosion potential, E_{corr}, is a measure of stability of the surface towards corrosion when immersed in corrosive media. From Figure 9, it was evident that bare NiTi alloy exhibited an active/passive transient behavior during anodic polarization. Similar transient peak was also observed by Hu et al. for bare NiTi alloy in 0.9% NaCl solution, while no such behavior could be noticed in case of treated samples [17]. Bare NiTi alloy revealed a corrosion potential of −0.47 V versus SCE. The breakdown of the passive film and the inception of pitting attack occurred at lower anodic potential of 0.49 V, indicated by sharp increase in current density for small change in potentials. The corrosion potential of all the treated samples was found to be nobler than untreated ones. An excellent biocompatible material should exhibit higher breakdown potential and minimum passive current density over a wide range of potentials which ensures good passivity at the surface [37]. The corrosion current density observed for bare NiTi was 7.7×10^{-7} Acm^{-2}. For all the treated samples there was almost two-magnitude decrease in corrosion current density which was in the order of 10^{-9} Acm^{-2}. Sun and Wang reported that, after the surface treatment on NiTi alloy, the corrosion current density was in the order of 10^{-6} Acm^{-2}

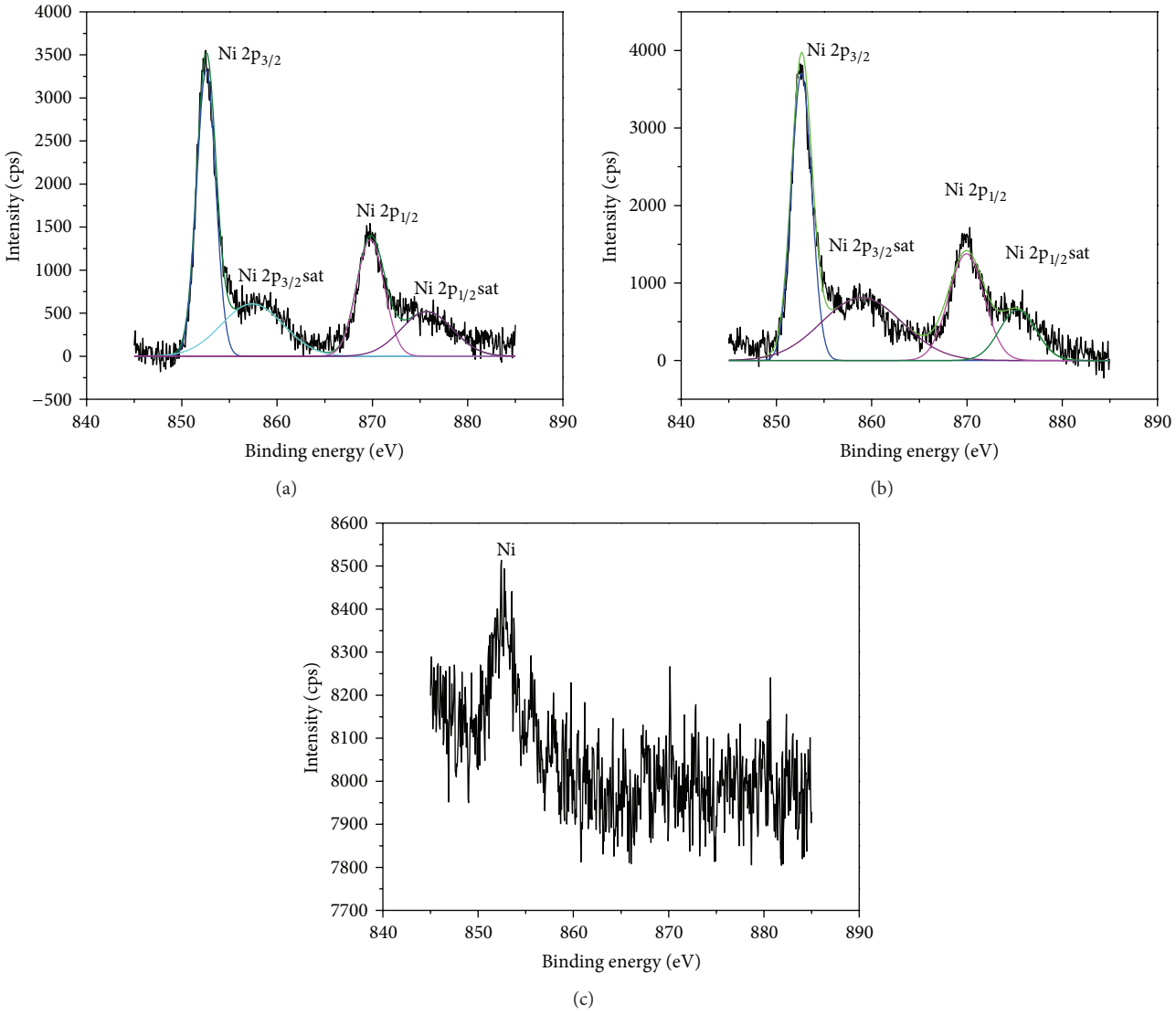

Figure 8: High resolution XPS spectra for Ni 2p region: (a) bare NiTi, (b) EP20V, and (c) EP20VPIE.

when analyzed in PBS solution [38]. The diversity in the physical, chemical, and electrochemical properties of NiTi alloy could be correlated to the differences in processing parameters and the composition of the alloy. The breakdown potential, E_b, of EP20V and EP20VPIE was 1140 mV and 1008 mV, respectively. The passive current density, i_b, for mechanically polished sample was 1.9×10^{-5} Acm^{-2}. There was one-order magnitude decrease in passive current density for EP20V. For EP20VPIE sample there was two-order magnitude decrease in passive current density; the value was around 3.6×10^{-7} Acm^{-2} signifying more passive behavior. In the biomedical application point of view, implanted material should retain its passivity to prevent the failure of the device. Several parameters influence the corrosion behavior of implanted material such as localized pH, temperature, tribological effect, and ionic concentrations. Hence, it can be expected that a stable and more passive surface can give better corrosion resistance for these applications. Therefore, from Figure 9 it was evident that passivation process after electropolishing resulted in lowering the corrosion current density and exhibited more noble corrosion potential. This indicates the effective improvement in the corrosion resistance performance due to the passivation treatment. For electropolished sample the anodic curve displayed active behavior until around 0.5 V and the formed passive layer was stable until 1.1 V. However, for passivated sample, the anodic curve exhibited passivity from 0 V which extended until 1 V. Therefore the range of passive behavior was the highest for passivated samples.

In PBS solution, mechanically polished NiTi alloy exhibited highest rate of corrosion (6.98×10^{-3} mm/year). In the case of electropolished and passivated samples, the rate of corrosion was in the order of 10^{-5} mm/year which was almost two orders lower than bare NiTi. This indicated that untreated alloy was more susceptible for corrosion than the samples subjected to electropolishing. The material loss due

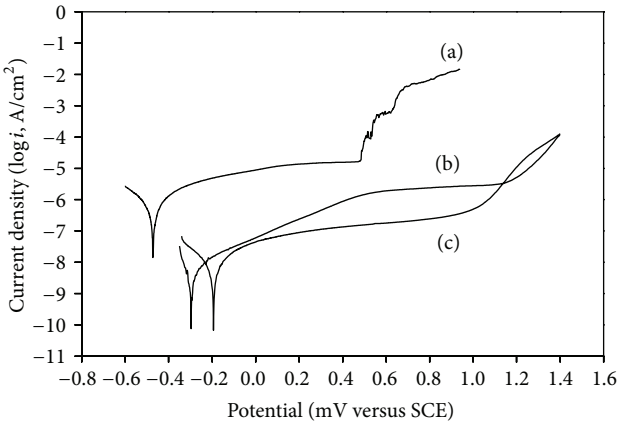

(a) MP NiTi
(b) EP20V
(c) EP20VPIE

Figure 9: Potentiodynamic polarization curves of untreated and treated alloys.

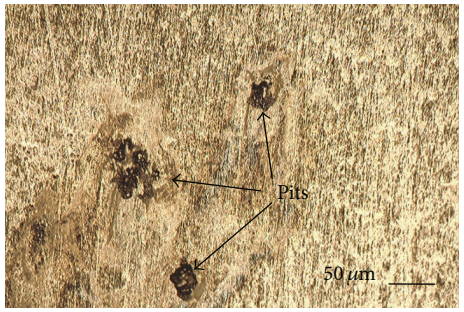

Figure 10: Optical micrograph of bare NiTi alloy after potentiodynamic polarization test.

to corrosion can be further reduced by passivation treatment in periodate solution.

The optical image of bare NiTi alloy after potentiodynamic polarization test is shown in Figure 10. Pits could be seen on the sample surface as a result of the attack of chloride ions present in the medium. Bare NiTi samples were more susceptible to pitting corrosion than the surface treated NiTi alloy. Pitting usually initiates whenever there is a defect in the native oxide layer. During polarization, once a pit is formed, the parent material gets exposed to the electrolyte solution. The inner anodic site is prone to corrosion, resulting in faster dissolution of the material. The polarization curves of the surface treated samples did not exhibit pitting type of corrosion, which means that the surface was nearly defect-free after electropolishing and passivation. These results suggest that electropolishing and passivation improve the corrosion resistance of NiTi alloy as indicated by more positive corrosion potential and lower corrosion current density.

Electrochemical impedance spectroscopy (EIS) studies are a useful technique which give quantitative information on the mechanism of corrosion of metals when immersed in an electrolytic solution. Figures 11(a)–11(c) show the Bode plots obtained from as-polished and surface treated NiTi alloy in PBS solution. These experimental results are fitted to appropriate equivalent circuits as shown in Figure 12.

In the circuit, R_s represents the electrolyte resistance between the working electrode and reference electrode, R_p is the double electrochemical layer resistance associated with the charge transfer resistance at the electrolyte-porous layer interface and C_p is its capacitance, R_b is resistance of the barrier layer, and C_b is barrier layer capacitance. In order to account for nonideal frequency response, it is commonly accepted to employ constant phase element (CPE) denoted by Q, which has a noninteger power dependence on the frequency, instead of pure capacitance. The impedance of a CPE is defined as

$$Z_{\mathrm{CPE}} = Y^{-1}\left(j\omega\right)^{-n}, \tag{2}$$

where Y is the proportional factor, j is $\sqrt{-1}$, ω is the frequency, and $-1 < n < 1$ has the meaning of a phase shift. If $n = 1$, Q is pure capacitance, and if $n = 0$, Q is pure resistance.

The equivalent circuit used for fitting the experimental data of the present study has been found to be similar to earlier proposed circuit for Ti and its alloys [39–41]. The fitting quality was evaluated by chi-square value which was found to be in the order of 10^{-3}-10^{-4} and the relative error values were below 10%. The fitting parameters used to simulate EIS data for NiTi alloy of different surface finishes are given in Table 6.

In the present study, a bell shaped Bode plot was obtained for bare NiTi (Figure 11(a)). Hang et al. reported similar behavior for NiTi substrate in PBS solution [42]. The electropolished and passivated alloys exhibited two-time constant behavior, consisting of outer porous layer whose resistance is R_p and an inner barrier layer whose resistance is R_b. These surfaces showed a typical behavior of a corrosion resistant surface exhibiting a near capacitive response as illustrated by a phase angle close to -90° over a wide range of frequencies, suggesting that a very stable passive film was formed after surface treatment of NiTi alloy with a double layer structure. The polarization resistance value of bare NiTi sample was given by $3.8 \times 10^4\ \Omega\mathrm{cm}^2$. The resistance of the porous layer for both electropolished and passivated samples was, respectively, 6.7 and $4.2\ \Omega\mathrm{cm}^2$. The barrier layer resistances of these samples were found to be in the order of $10^6\ \Omega\mathrm{cm}^2$. Therefore the outer porous layer was not efficient in preventing the attack of corrosive ions but the inner barrier layer could withstand their attack. There was 100 times increase in polarization resistance ($R_p + R_b$) values for all the surface treated alloys in comparison with untreated alloys, indicating that electropolishing and passivation can control the charge transfer at substrate/electrolyte interface and hence improved the corrosion resistance. Further the R_b value for the passivated sample was almost three times higher than electropolished samples. In general, the term "n" signifies the surface roughness of the working electrode. The deviation of "n" from unity indicates an uneven surface finish. The "n" value was found to be the least (Table 6) for passivated samples due to the chemical reaction at the solution/sample

Table 6: Fitted values for simulative EIS spectra of untreated and treated alloys.

Sample	Circuit	Q_p (Ss^ncm^{-2})	n	R_p (Ωcm^2)	Q_b (Ss^ncm^{-2})	n	R_b (Ωcm^2)
Bare NiTi	$R(QR)$				3.6×10^{-5}	0.94	$3.8 \times 10^{+4}$
EP20V	$R(Q(R(QR)))$	4.2×10^{-7}	0.94	6.718	7.9×10^{-6}	0.96	$1.2 \times 10^{+6}$
EP20VPIE	$R(Q(R(QR)))$	5.4×10^{-6}	0.98	4.2	4.3×10^{-7}	0.88	$3.0 \times 10^{+6}$

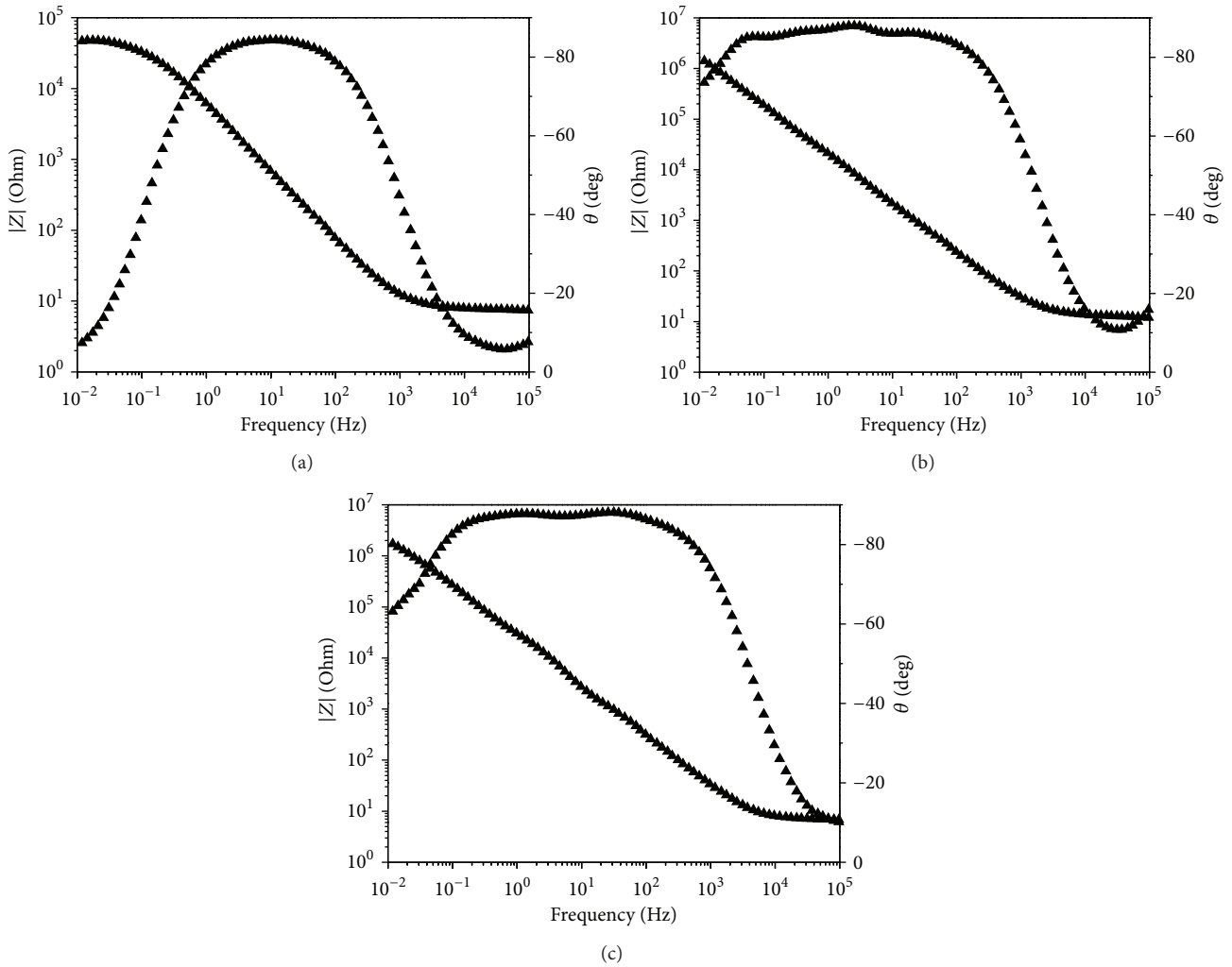

Figure 11: Bode plots of NiTi alloy with various surface treatments: (a) bare NiTi, (b) EP20V, and (c) EP20VPIE.

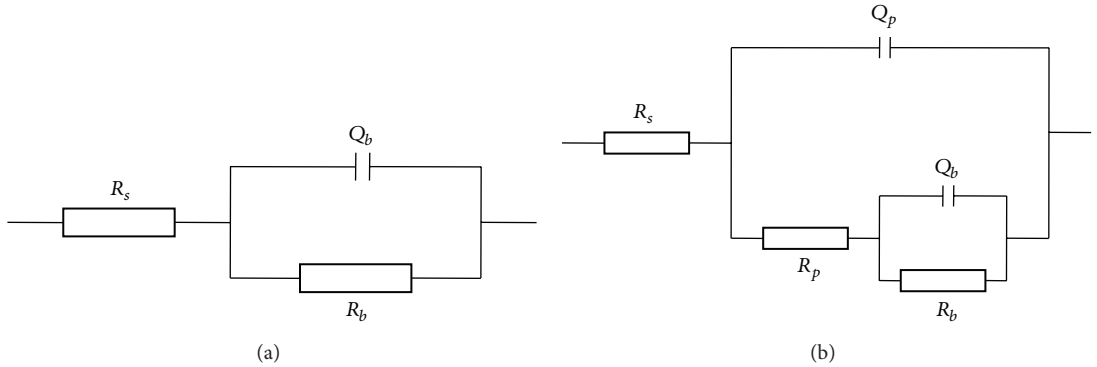

Figure 12: Equivalent circuit for the interpretation of experimental Bode diagrams of (a) bare NiTi and (b) electropolished and passivated alloys.

interface which modified the surface finish. The R_a value obtained from AFM studies also confirmed a rougher surface after post-treatment.

The barrier layer capacitance, Q_b, for bare NiTi, EP20V, and EP20VPIE was 36, 7.9, and 0.43 $\mu Ss^n cm^{-2}$, respectively, which means that the thickness of the barrier layer formed after mechanical polishing was very thin compared to surface treated alloys. The capacitance, C, and the thickness, d, are related by the equation $C = \varepsilon\varepsilon_0 A/d$, where ε is the dielectric constant of the barrier, ε_0 the vacuum permittivity, A the area, and d the thickness of the oxide layer. Therefore the higher the capacitance, the lower the thickness of the oxide formed. The oxide layer thickness increased almost 85 times after electropolishing and passivation when compared to mechanically polished samples. The barrier layer resistance, R_b, also gave the same conclusion, in which the barrier layer resistance of bare NiTi was almost 100 times lower than that of surface treated alloys. The thickness of the oxide layer of passivated samples was almost 18 times higher than electropolished samples. This indicated better protection capacity of the oxide formed after post-treatment.

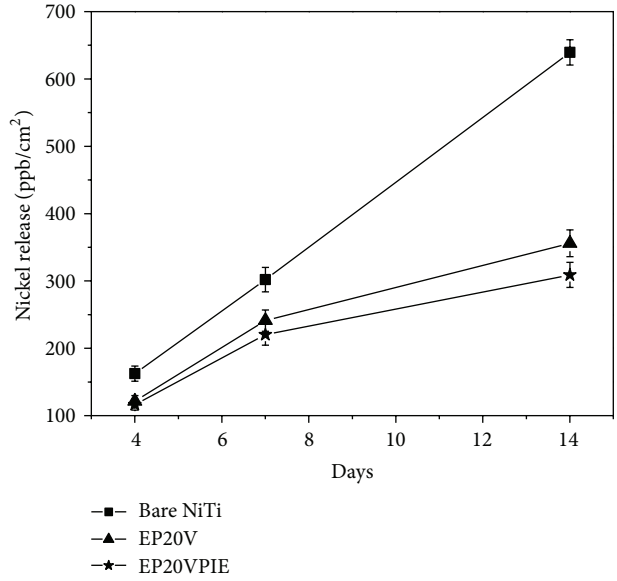

Figure 13: Nickel ion release measured as a function of immersion duration in Hanks' solution.

3.5. Nickel Release. Surface modification by electropolishing process aids in removing the defective passive layer and due to the formation of uniform surface a more homogenous passive layer will be formed which can effectively prevent the release of nickel. The results of cumulative nickel release rate measured as a function of immersion duration in Hanks' solution for a period of 14 days were given in Figure 13.

It was evident from Figure 13 that electropolishing process significantly reduced the nickel elution compared to bare NiTi. Passivated NiTi alloy showed lowest nickel ion release. The trend in release rate was altered due to surface modification even though it could not completely prevent the nickel elution. For bare NiTi alloy, the amount of nickel eluted was 640 ppb after 2 weeks of immersion. Passivated surface which has the lowest water contact angle showed minimal amount of nickel release among all the samples. This may be due to the increase in the thickness and/or compactness of the passive titania layer which reduced the harmful nickel elution.

Native titanium oxide would be formed spontaneously on the surface of fresh cut NiTi alloy due to surface oxidation even at ambient conditions. After mechanical polishing, the surface possesses several scratch defects. The native oxide formed on NiTi alloy may not be uniform due to the presence of such defects. Electropolishing process aids in forming a homogenous surface and so the oxide layer formed would be almost defect free. During the process of electropolishing, because of the applied potential, a polishing film will form at the anode surface which controls the anodic dissolution of the substrate. Peaks which receive higher current densities will be selectively etched compared to the valleys resulting in a smooth surface finish. Along with anodic dissolution, oxygen evolution will also occur at the anode. Various reactions occurring at the electrodes during electropolishing can be written as

$$\begin{aligned} &2H_2O\,(aq) \\ &\quad \longrightarrow O_2\,(g) + 4H^+\,(aq) + 4e^- \quad \text{(Anodic oxidation)} \\ &2H_2O\,(aq) + 2e^- \\ &\quad \longrightarrow H_2\,(g) + 2OH^-\,(aq) \quad \text{(Cathodic reduction)} \end{aligned} \tag{3}$$

Nickel existing in nonoxidized state is more liable to dissolution and oxidation [34]. Initial reaction at the anode will be field assisted dissolution which may result in the migration of titanium and nickel ions to the polishing film/electrolyte interface and it chemically dissolves in perchloric acid:

$$\begin{aligned} TiO^{2+} + 4ClO_4{}^- &\longrightarrow Ti\,(ClO_4)_4 + \frac{1}{2}O_2 + 2e^- \\ Ni^{2+} + 2ClO_4{}^- &\longrightarrow Ni\,(ClO_4)_2 \end{aligned} \tag{4}$$

Due to the applied field, the outward diffusion of nickel from the substrate surface will be more and hence the electrolytic solution will be enriched with nickel and NiTi alloy surface with titanium even though the bulk composition remains unchanged.

Electropolished and passivated samples after polarization test did not show any pits at the surface, which is a characteristic feature of an inclusion/precipitate free surface. Passivation using saturated potassium periodate at 95°C resulted in the oxidation of NiTi alloy. The improved surface oxidation of NiTi alloy was also evident in the AFM images in which the nanosize peaks formed after electropolishing were converted to microsize peaks after passivation. Capacitive behavior over a wide range of frequencies supported the compactness of the oxide layer formed although some amount of unoxidized

titanium existed at the surface of the electropolished sample. Passivating the electropolished samples in periodate solution assisted in the complete oxidation of titanium to titania and hence the compactness of the oxide was further enhanced. This was also supported by *in vitro* nickel release analysis which showed that, due to passivation, nickel ion release was significantly reduced when compared to untreated NiTi alloy.

The present study established that electropolishing and postpassivation treatment result in a remarkable increase in the corrosion resistance and biocompatibility of NiTi alloy. The study was mainly focused on establishing the electrochemical behavior of the surface modified alloy on exposure to simulated body fluids for short term period. But from a biomaterial application point of view, the material needs to be evaluated further for its electrochemical behavior and nickel release rate on exposure to longer time duration. Another important aspect of the use of these materials for implant applications requires establishing osseointegration. An understanding of osseointegration behavior can be achieved by studying the growth characteristics of hydroxyapatite on the NiTi alloy surface on exposure to simulated body fluids and these studies show a great promise for future research.

4. Conclusions

In the present study, electropolishing of equiatomic NiTi alloy was carried out using perchloric acid based solution. Good electropolished surface was obtained within a short duration of 30 sec. Passivation at 95°C using potassium periodate solution improved the hydrophilicity of the alloy due to the formation of microsized nodules distributed over the surface. The passive film formed after surface treatment was more compact and uniform and no pits could be noticed as observed for mechanically polished samples. The Ti/Ni ratio substantially increased after passivation. The nickel content at the surface of the passivated sample was the least and hence the amount of nickel eluted out was also minimum. The barrier layer resistance increased thrice when compared to electropolished samples due to the increased stability of the oxide layer formed after passivation. Electropolishing in perchloric acid based electrolyte and passivation in potassium periodate solution would be beneficial for enhancing the biomedical properties of NiTi shape memory alloys.

Conflict of Interests

The authors declare that there is no conflict of interests regarding the publication of this paper.

Acknowledgments

The authors thank the Director, NAL, Council of Scientific and Industrial Research (CSIR), New Delhi, for giving permission to publish this work. The authors also thank present and past Heads, SED, for the support. The authors wish to thank Dr. S. K. Bhaumik and his group for providing the NiTi alloy used in this study. Help received from Mr. Praveen Kumar V for AFM, Mrs. Premlatha for surface roughness measurement, Mr. Srinivas G for XRD, Mr. Siju for SEM, Mr. Bharathidasan T for contact angle measurements, Dr. Parthasarathi Bera for XPS, and Mrs. Anila Kumari for AAS is greatly appreciated. One of the authors (Manju Chembath) acknowledges the financial assistance in the form of Senior Research Fellowship from CSIR-National Aerospace Laboratories, India.

References

[1] M. Es-Souni, M. Es-Souni, and H. Fischer-Brandies, "Assessing the biocompatibility of NiTi shape memory alloys used for medical applications," *Analytical and Bioanalytical Chemistry*, vol. 381, no. 3, pp. 557–567, 2005.

[2] C. Trepanier, R. Venugopalan, and A. R. Pelton, *Shape Memory Implants*, edited by L. Yahia, NDC, 2000.

[3] P. Rocher, L. El Medawar, J.-C. Hornez, M. Traisnel, J. Breme, and H. F. Hildebrand, "Biocorrosion and biocompatibility of NiTi alloys," *European Cells and Materials*, vol. 9, no. 1, pp. 23–24, 2005.

[4] B. Yuan, M. Lai, Y. Gao, C. Y. Chung, and M. Zhu, "The effect of pore characteristics on Ni suppression of porous NiTi shape memory alloys modified by surface treatment," *Thin Solid Films*, vol. 519, no. 15, pp. 5297–5301, 2011.

[5] Z. D. Cui, H. C. Man, and X. J. Yang, "The corrosion and nickel release behavior of laser surface-melted NiTi shape memory alloy in Hanks' solution," *Surface and Coatings Technology*, vol. 192, no. 2-3, pp. 347–353, 2005.

[6] S. A. Bernard, V. K. Balla, N. M. Davies, S. Bose, and A. Bandyopadhyay, "Bone cell-materials interactions and Ni ion release of anodized equiatomic NiTi alloy," *Acta Biomaterialia*, vol. 7, no. 4, pp. 1902–1912, 2011.

[7] L. A. Bravo, A. G. de Cabañes, J. M. Manero, E. Rúperez, and F. J. Gil, "NiTi superelastic orthodontic archwires with polyamide coating," *Journal of Materials Science: Materials in Medicine*, vol. 25, no. 2, pp. 555–560, 2014.

[8] F. Sun, K. N. Sask, J. L. Brash, and I. Zhitomirsky, "Surface modifications of Nitinol for biomedical applications," *Colloids and Surfaces B: Biointerfaces*, vol. 67, no. 1, pp. 132–139, 2008.

[9] Y. Cheng and Y. F. Zheng, "The corrosion behavior and hemocompatibility of TiNi alloys coated with DLC by plasma based ion implantation," *Surface and Coatings Technology*, vol. 200, no. 14-15, pp. 4543–4548, 2006.

[10] W. Simka, M. Kaczmarek, A. Baron-Wiecheć, G. Nawrat, J. Marciniak, and J. Żak, "Electropolishing and passivation of NiTi shape memory alloy," *Electrochimica Acta*, vol. 55, no. 7, pp. 2437–2441, 2010.

[11] M. Kaczmarek, W. Simka, A. Baron, J. Szewczenko, and J. Marciniak, "Electrochemical behavior of Ni-Ti alloy after surface modification," *Journal of Achievements in Materials and Manufacturing Engineering*, vol. 18, pp. 111–114, 2006.

[12] W. Wu, X. Liu, H. Han, D. Yang, and S. Lu, "Electropolishing of NiTi for improving biocompatibility," *Journal of Materials Science and Technology*, vol. 24, no. 6, pp. 926–930, 2008.

[13] G. Bolat, D. Mareci, S. Iacoban, N. Cimpoesu, and C. Munteanu, "The estimation of corrosion behavior of NiTi and NiTiNb alloys using dynamic electrochemical impedance spectroscopy," *Journal of Spectroscopy*, vol. 2013, Article ID 714920, 7 pages, 2013.

[14] B. G. Pound, "Susceptibility of nitinol to localized corrosion," *Journal of Biomedical Materials Research Part A*, vol. 77, no. 1, pp. 185–191, 2006.

[15] W. Haider and N. Munroe, "Assessment of corrosion resistance and metal ion leaching of nitinol alloys," *Journal of Materials Engineering and Performance*, vol. 20, no. 4-5, pp. 812–815, 2011.

[16] R. A. Silva, I. P. Silva, and B. Rondot, "Effect of surface treatments on anodic oxide film growth and electrochemical properties of tantalum used for biomedical applications," *Journal of Biomaterials Applications*, vol. 21, pp. 93–103, 2006.

[17] T. Hu, Y. C. Xin, S. L. Wu et al., "Corrosion behavior on orthopedic NiTi alloy with nanocrystalline/amorphous surface," *Materials Chemistry and Physics*, vol. 126, no. 1-2, pp. 102–107, 2011.

[18] W. Haider, N. Munroe, C. Pulletikurthi, P. K. S. Gill, and S. Amruthaluri, "A comparative biocompatibility analysis of ternary nitinol alloys," *Journal of Materials Engineering and Performance*, vol. 18, no. 5-6, pp. 760–764, 2009.

[19] O. Cisse, O. Savadogo, M. Wu, and L. H. Yahia, "Effect of surface treatment of NiTi alloy on its corrosion behavior in Hanks' solution," *Journal of Biomedical Materials Research*, vol. 61, no. 3, pp. 339–345, 2002.

[20] T. Hryniewicz, "Concept of microsmoothing in electropolishing process," *Surface & Coatings Technology*, vol. 64, no. 2, pp. 75–80, 1994.

[21] L. Neelakantan, M. Valtiner, G. Eggeler, and A. W. Hasse, "Surface chemistry and topographical changes of an electropolished NiTi shape memory alloy," *Physica Status Solidi (A) Applications and Materials Science*, vol. 207, no. 4, pp. 807–811, 2010.

[22] C. L. Chu, R. M. Wang, T. Hu et al., "Surface structure and biomedical properties of chemically polished and electropolished NiTi shape memory alloys," *Materials Science and Engineering C*, vol. 28, no. 8, pp. 1430–1434, 2008.

[23] D. Batalu and H. Guoqiu, "Improvement of the corrosion resistance of equiatomic NiTi shape memory alloy for medical implants by the electropolishing method," *UPB Scientific Bulletin B*, vol. 71, p. 832, 2009.

[24] K. Fushimi, M. Stratmann, and A. W. Hassel, "Electropolishing of NiTi shape memory alloys in methanolic H_2SO_4," *Electrochimica Acta*, vol. 52, no. 3, pp. 1290–1295, 2006.

[25] F. Feigl and V. Anger, *Spot Tests in Inorganic Analysis*, Elsevier Science BV, Amsterdam, The Netherlands, 6th edition, 2012.

[26] J.-X. Liu, D.-Z. Yang, F. Shi, and Y.-J. Cai, "Sol-gel deposited TiO_2 film on NiTi surgical alloy for biocompatibility improvement," *Thin Solid Films*, vol. 429, no. 1-2, pp. 225–230, 2003.

[27] J. H. Yu, L. C. Wu, J. T. Hsu, Y. Y. Chang, H. H. Huang, and H. L. Huang, "Surface roughness and topography of four commonly used types of orthodontic archwire," *Journal of Medical and Biological Engineering*, vol. 31, no. 5, pp. 367–370, 2011.

[28] N. Eliaz and O. Nissan, "Innovative processes for electropolishing of medical devices made of stainless steels," *Journal of Biomedical Materials Research A*, vol. 83, no. 2, pp. 546–557, 2007.

[29] F. L. Nie, Y. F. Zheng, Y. Cheng, S. C. Wei, and R. Z. Valiev, "In vitro corrosion and cytotoxicity on microcrystalline, nanocrystalline and amorphous NiTi alloy fabricated by high pressure torsion," *Materials Letters*, vol. 64, no. 8, pp. 983–986, 2010.

[30] T. Hu, C.-L. Chu, L.-H. Yin et al., "*In vitro* biocompatibility of titanium-nickel alloy with titanium oxide film by H_2O_2 oxidation," *Transactions of Nonferrous Metals Society of China*, vol. 17, no. 3, pp. 553–557, 2007.

[31] X. Zhu, J. Chen, L. Scheideler, R. Reichl, and J. Geis-Gerstorfer, "Effects of topography and composition of titanium surface oxides on osteoblast responses," *Biomaterials*, vol. 25, no. 18, pp. 4087–4103, 2004.

[32] C. C. Annarelli, J. Fornazero, R. Cohen, J. Bert, and J.-L. Besse, "Colloidal protein solutions as a new standard sensor for adhesive wettability measurements," *Journal of Colloid and Interface Science*, vol. 213, no. 2, pp. 386–394, 1999.

[33] Z. Huan, L. E. Fratila-Apachitei, I. Apachitei, and J. Duszczyk, "Porous NiTi surfaces for biomedical applications," *Applied Surface Science*, vol. 258, no. 13, pp. 5244–5249, 2012.

[34] D. Vojtěch, J. Fojt, L. Joska, and P. Novák, "Surface treatment of NiTi shape memory alloy and its influence on corrosion behavior," *Surface and Coatings Technology*, vol. 204, no. 23, pp. 3895–3901, 2010.

[35] D. Vojtech, M. Voderova, J. Fojt, P. Novak, and T. Kubasek, "Surface structure and corrosion resistance of short-time heat-treated NiTi shape memory alloy," *Applied Surface Science*, vol. 257, no. 5, pp. 1573–1582, 2010.

[36] D. R. Lide, *CRC Handbook of Chemistry and Physics*, Taylor & Francis Group, Boca Raton, Fla, USA, 89th edition, 2008.

[37] X.-J. Yan and D.-Z. Yang, "Corrosion resistance of a laser spot-welded joint of Ni-Ti wire in simulated human body fluids," *Journal of Biomedical Materials Research*, vol. 77, no. 1, pp. 97–102, 2006.

[38] T. Sun and M. Wang, "A comparative study on titania layers formed on Ti, Ti-6Al-4V and NiTi shape memory alloy through a low temperature oxidation process," *Surface and Coatings Technology*, vol. 205, no. 1, pp. 92–101, 2010.

[39] H. Maleki-Ghaleh, V. Khalili, J. Khalil-Allafi, and M. Javidi, "Hydroxyapatite coating on NiTi shape memory alloy by electrophoretic deposition process," *Surface and Coatings Technology*, vol. 208, pp. 57–63, 2012.

[40] I. Milošev, T. Kosec, and H.-H. Strehblow, "XPS and EIS study of the passive film formed on orthopaedic Ti-6Al-7Nb alloy in Hank's physiological solution," *Electrochimica Acta*, vol. 53, no. 9, pp. 3547–3558, 2008.

[41] M. Attarchi, M. Mazloumi, I. Behckam, and S. K. Sadrnezhaad, "EIS study of porous NiTi biomedical alloy in simulated body fluid," *Materials and Corrosion*, vol. 60, no. 11, pp. 871–875, 2009.

[42] R. Hang, S. Ma, and P. K. Chu, "Corrosion behavior of DLC-coated NiTi alloy in the presence of serum proteins," *Diamond and Related Materials*, vol. 19, no. 10, pp. 1230–1234, 2010.